

Supplementary Information

Tuning the Confinement Space of N-Carbon Shell-Coated Ruthenium Nanoparticles: Highly Efficient Electrocatalysts for Hydrogen Evolution Reaction

Xianlang Chen,^a Jian Zheng,^a Xing Zhong*,^a Yihang Jin,^a Guilin Zhuang,^a Xiaonian Li,^a Shengwei Deng^a and Jian-guo Wang*^a

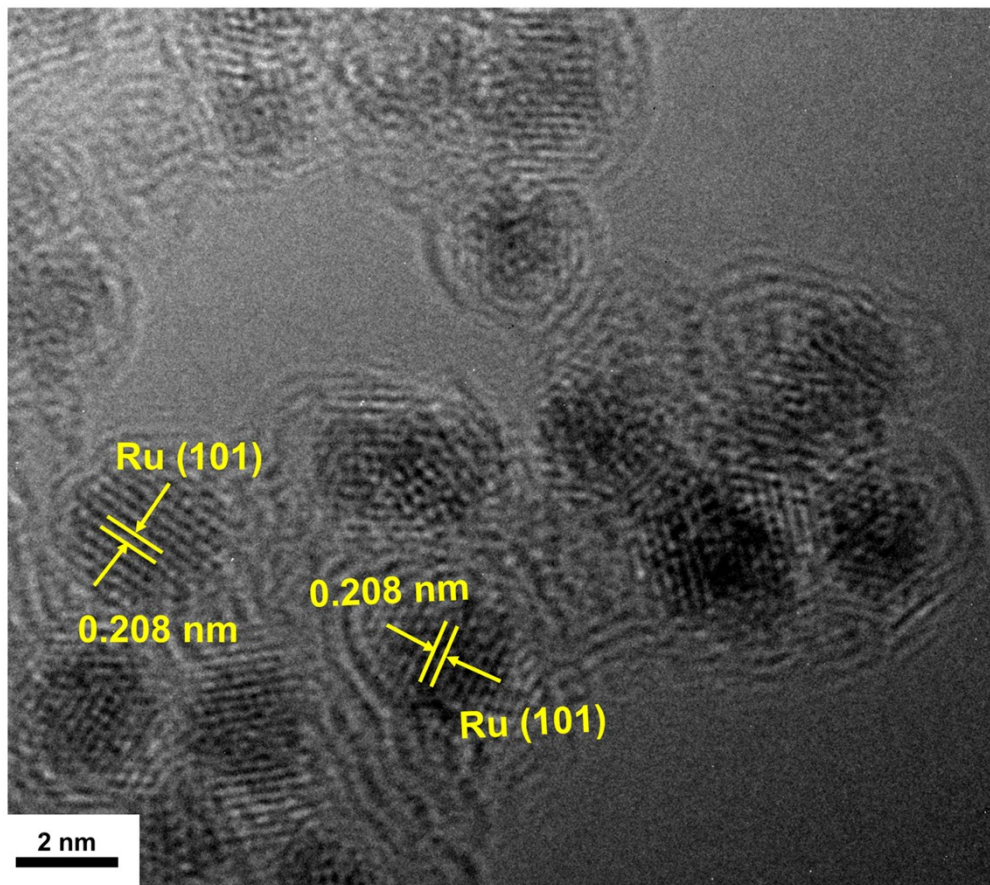


Figure S1. HRTEM images of 5.0% F-Ru@PNC-800, showing the graphene shells and encapsulated metal nanoparticles.

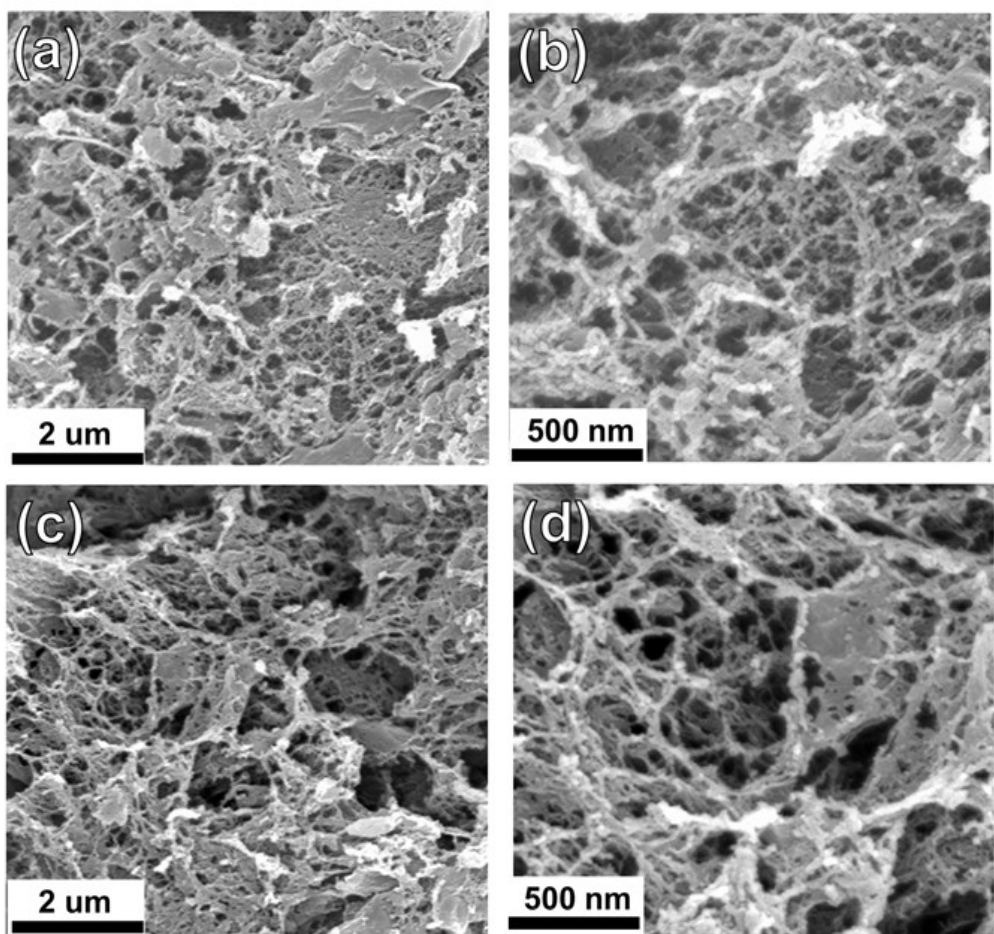


Figure S2. SEM images of (a, b) 2.5% F-Ru@PNC-800 (c, d) 7.5% F-Ru@PNC-800.

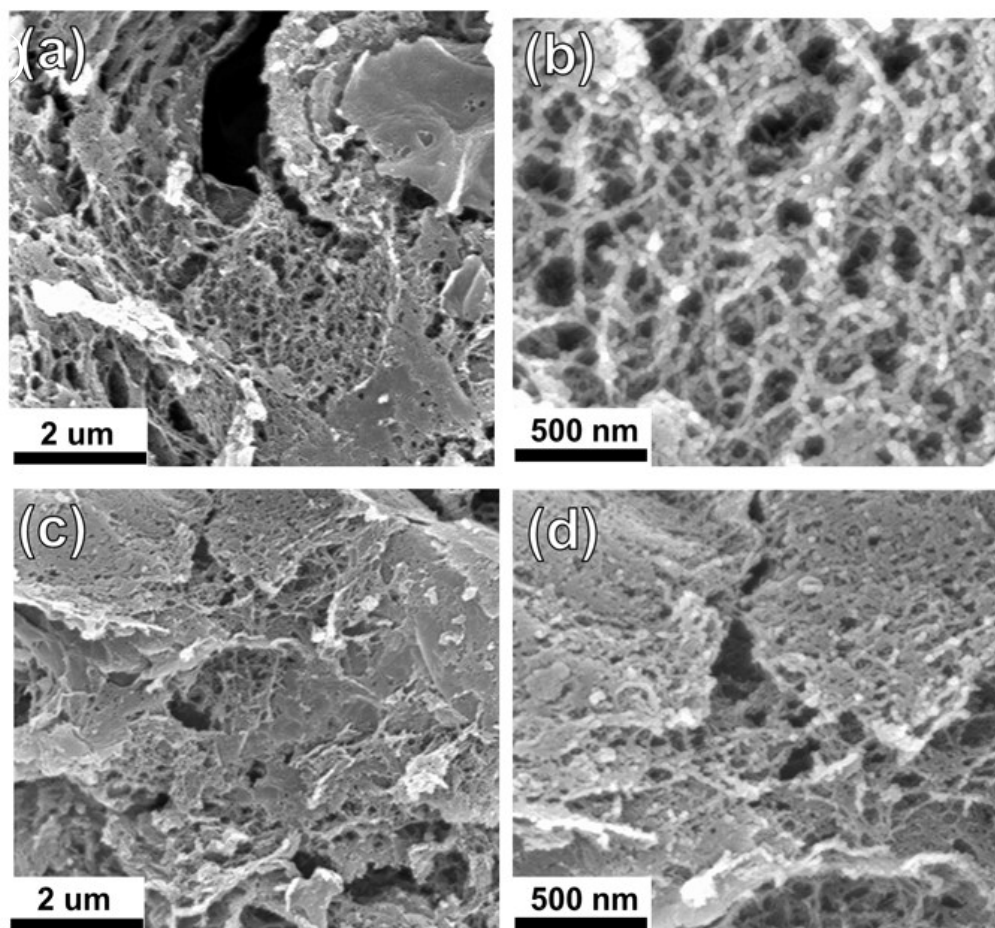


Figure S3. SEM images of (a, b) 5.0% F-Ru@PNC-700 (c, d) 5.0% F-Ru@PNC-900.

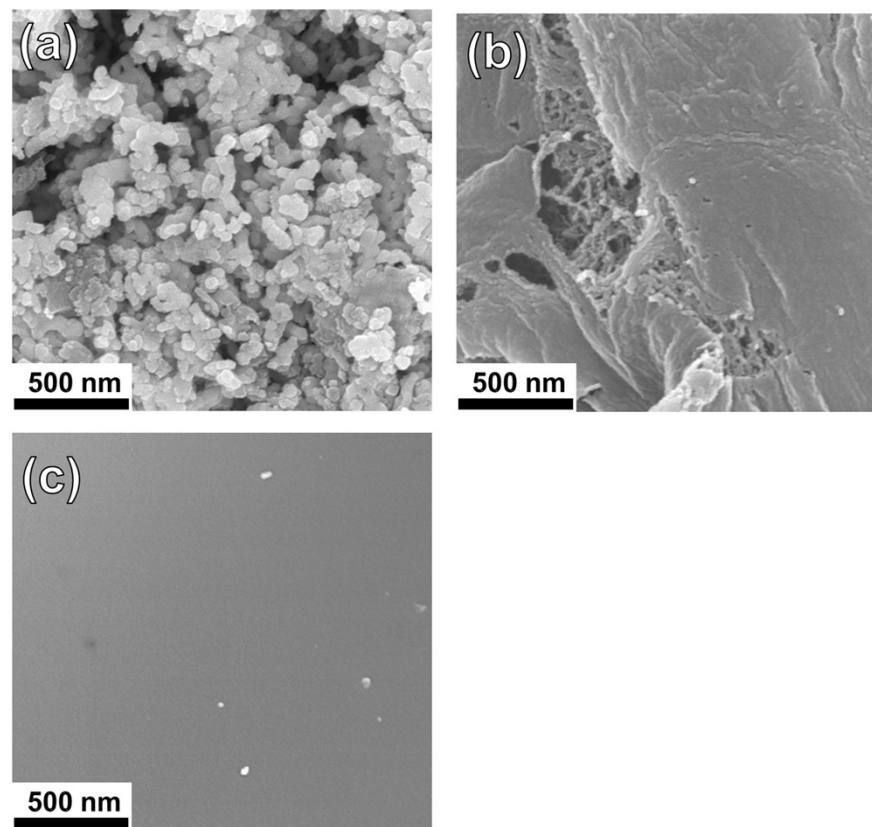


Figure S4. SEM images of the samples obtained with different precursors: (a) No glucose, (b) No $(\text{NH}_4)_2\text{SO}_4$ and (c) No DCDA.

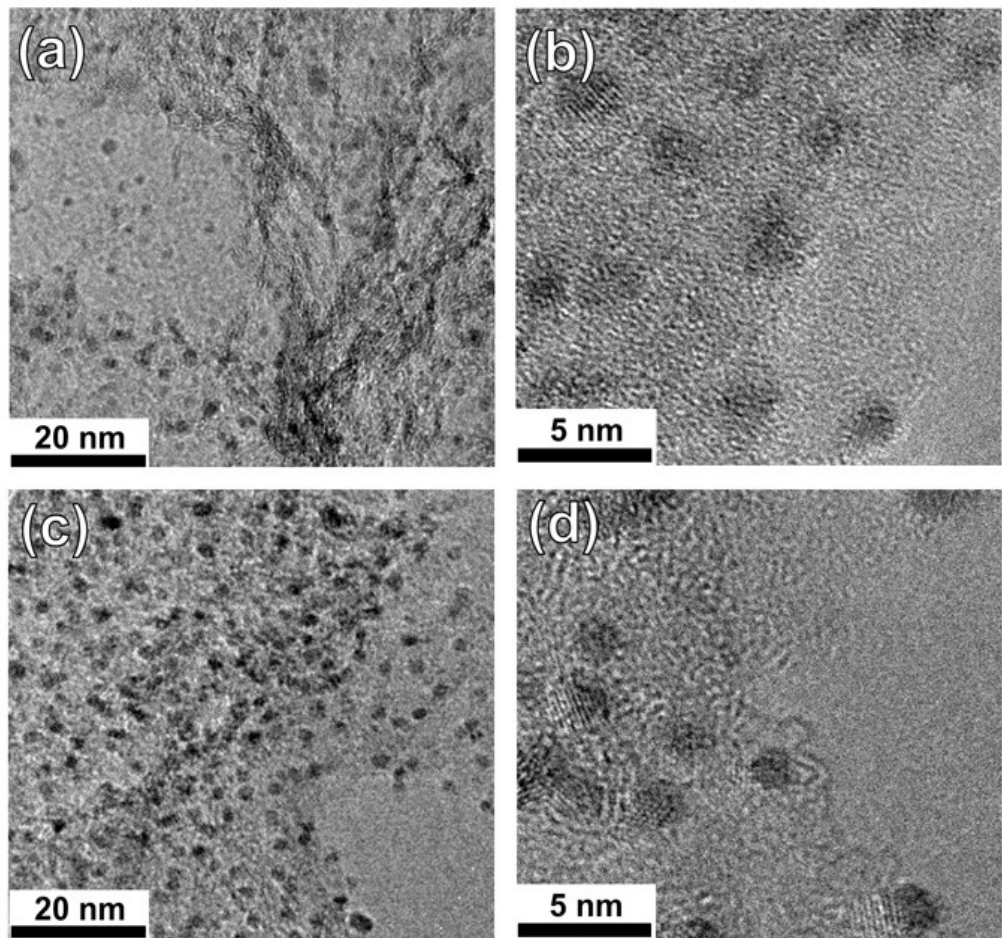


Figure S5. TEM image of (a, b) 2.5% F-Ru@PNC-800 (c, d) 7.5% F-Ru@PNC-800.

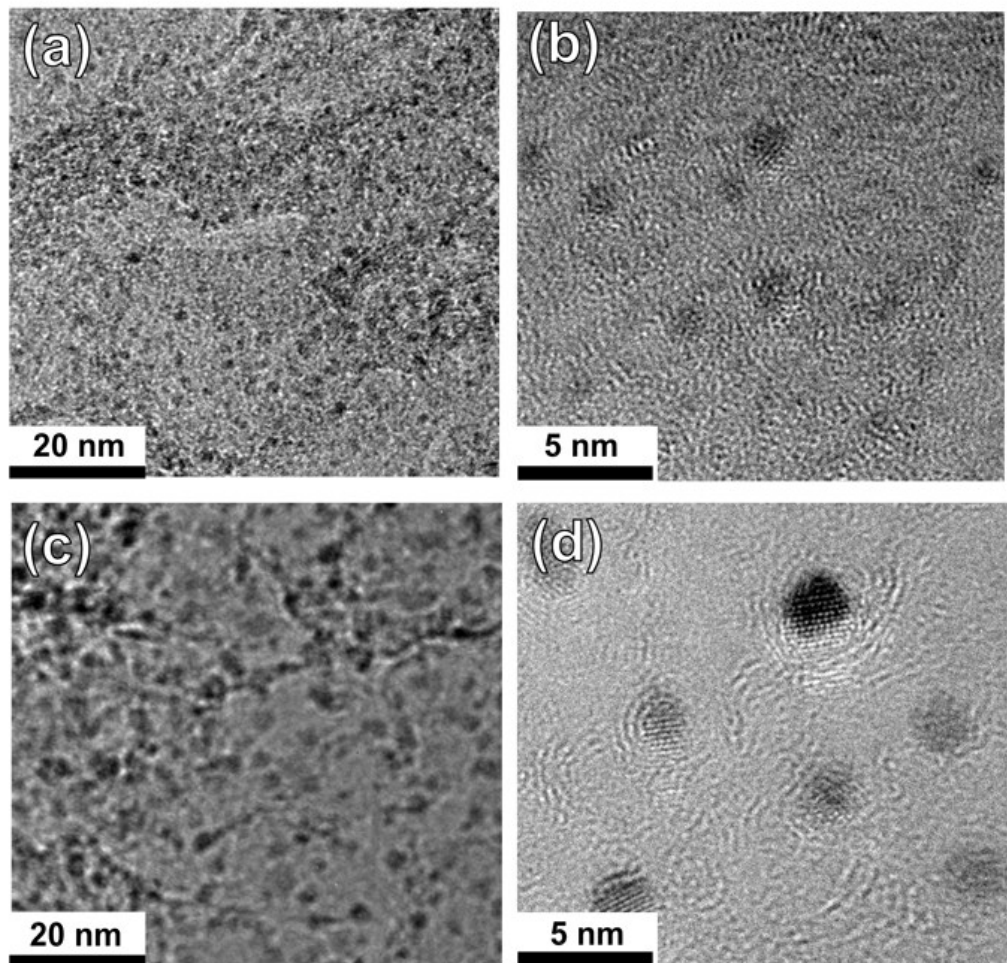


Figure S6. TEM image of (a, b) 5.0% F-Ru@PNC-700 (c, d) 5.0% F-Ru@PNC-900.

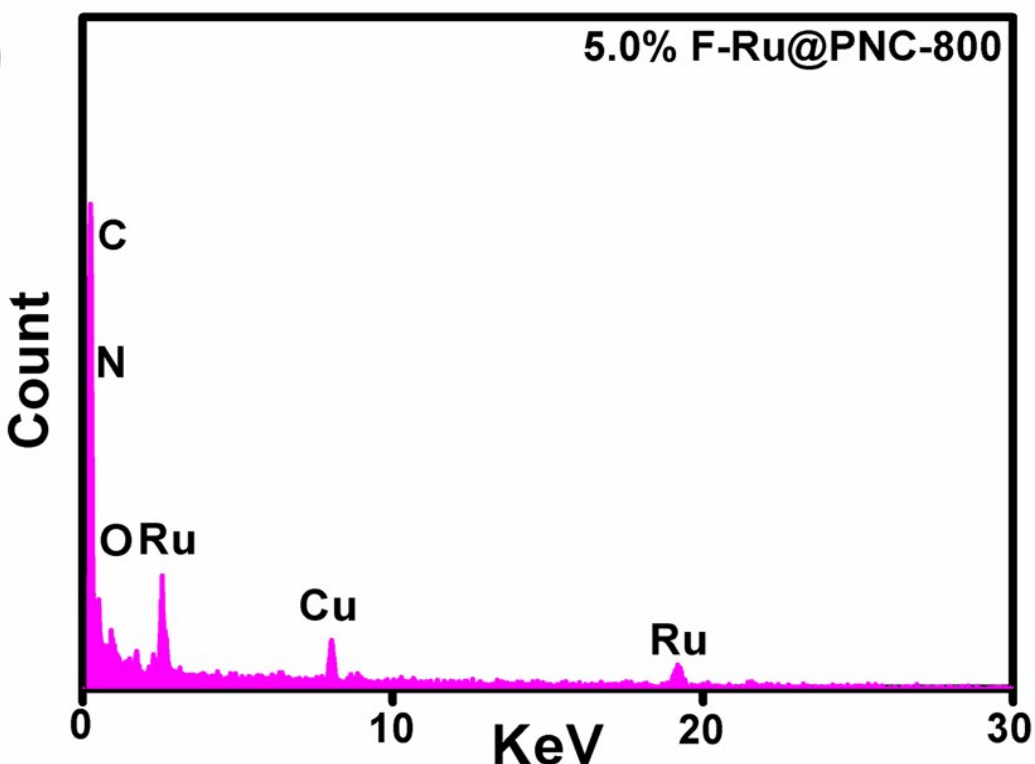


Figure S7. EDS spectrum of 5.0% F-Ru@PNC-800.

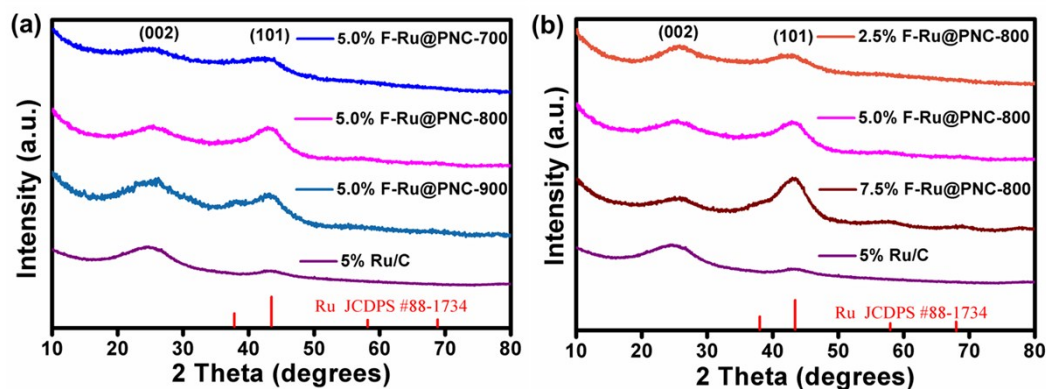


Figure S8. XRD patterns of (a) F-Ru@PNC-800 samples obtained at different content and commerce Ru/C (b) 5.0% F-Ru@PNC samples obtained at different temperatures and commerce Ru/C.

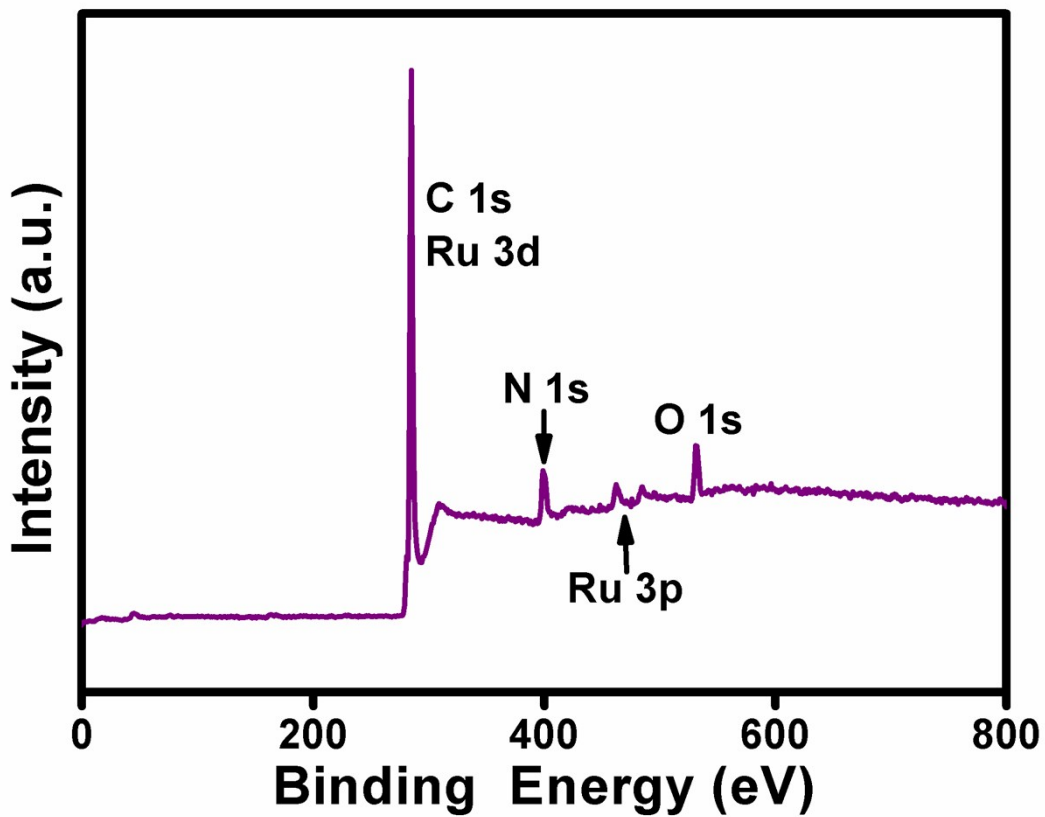


Figure S9. XPS spectrum of 5.0% F-Ru@PNC-800.

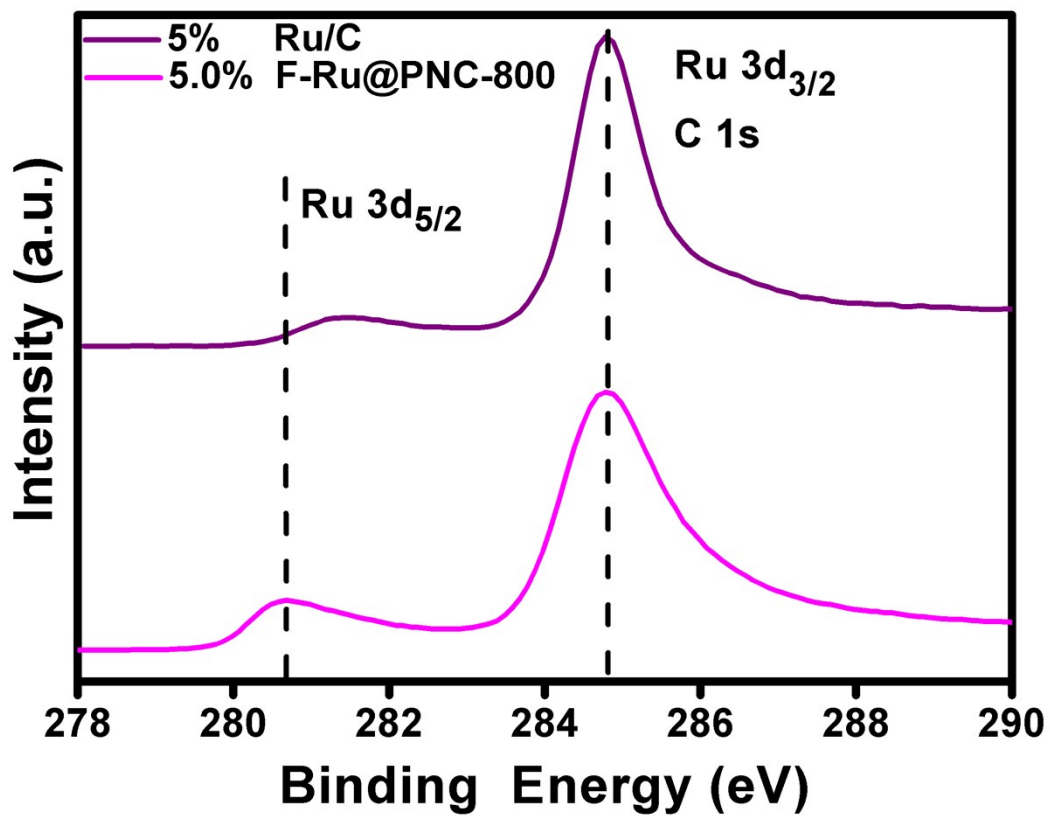


Figure S10. XPS spectrum of Ru 3d spectral region for 5% Ru/C and 5.0% F-Ru@PNC-800.

Table S1. Element analysis results of the F-Ru@PNC-800 samples with different content.

Samples	Ru (at %)	C (at %)	N (at %)	O (at %)
2.5% Ru@PNC-800	0.3	85.94	8.82	4.94
5.0% Ru@PNC-800	0.63	81.97	9.91	7.49
7.5% Ru@PNC-800	0.97	84.14	9.41	5.48

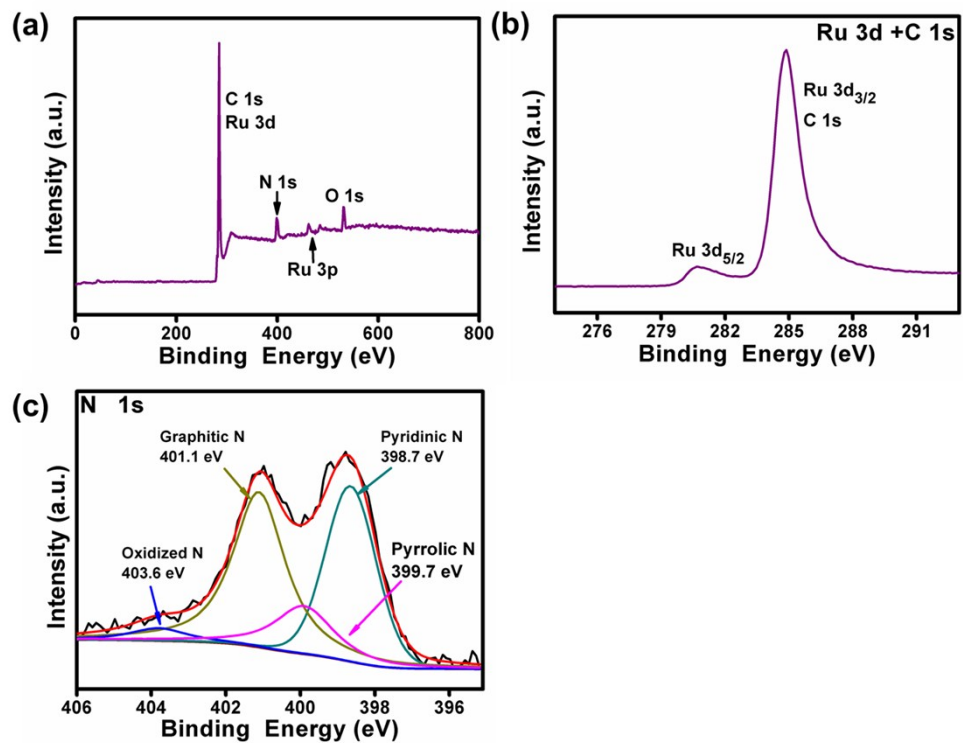


Figure S11. XPS spectrum of (a) 2.5% F-Ru@PNC-800 (b) Ru 3d spectral region for 2.5% F-Ru@PNC-800 (c) N 1s spectral region for 2.5% F-Ru@PNC-800.

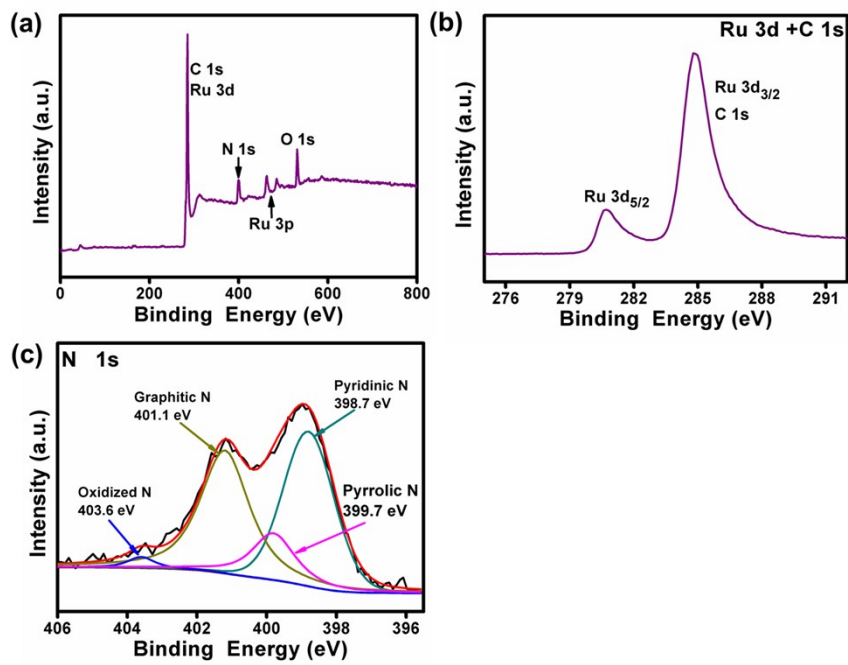


Figure S12. XPS spectrum of (a) 7.5% F-Ru@PNC-800 (b) Ru 3d spectral region for 7.5% F-Ru@PNC-800 (c) N 1s spectral region for 7.5% F-Ru@PNC-800.

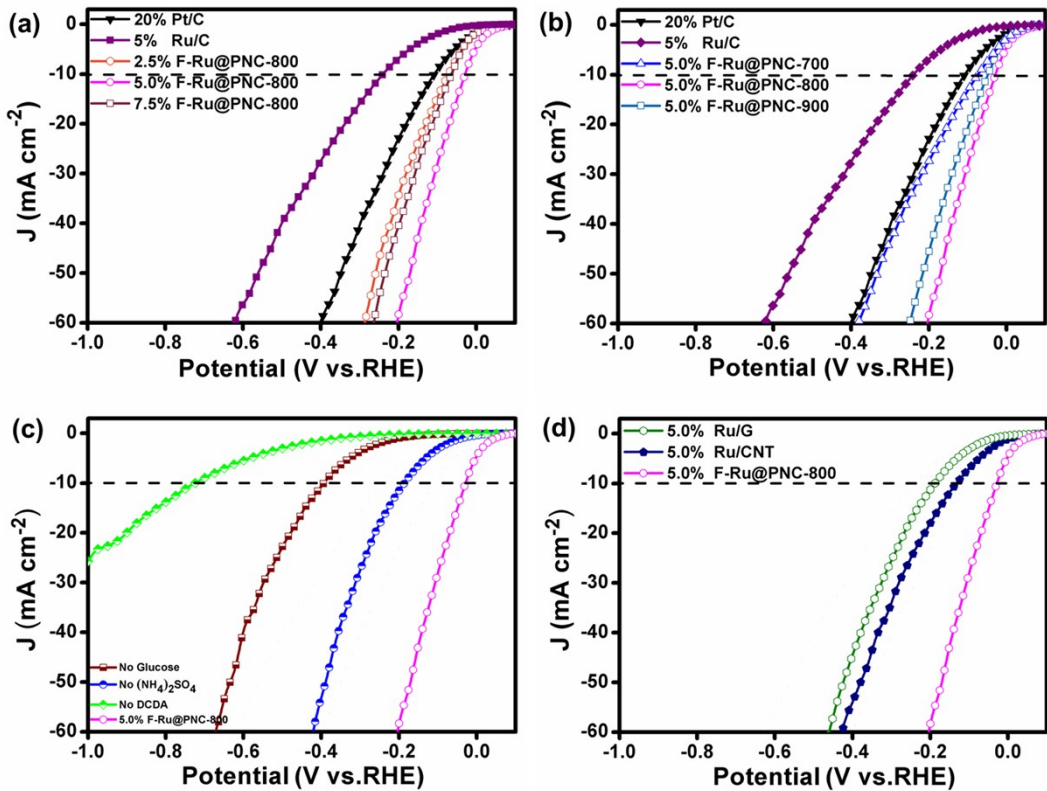


Figure S13. The HER polarization curves of (a) F-Ru@PNC-800 at different content, commerce Ru/C and Pt/C in 0.1 M KOH (b) 5.0% F-Ru@PNC at different temperatures, commerce Ru/C and Pt/C in 0.1 M KOH (c) different precursors in 0.1 M KOH (d) different dimensions in 0.1 M KOH.

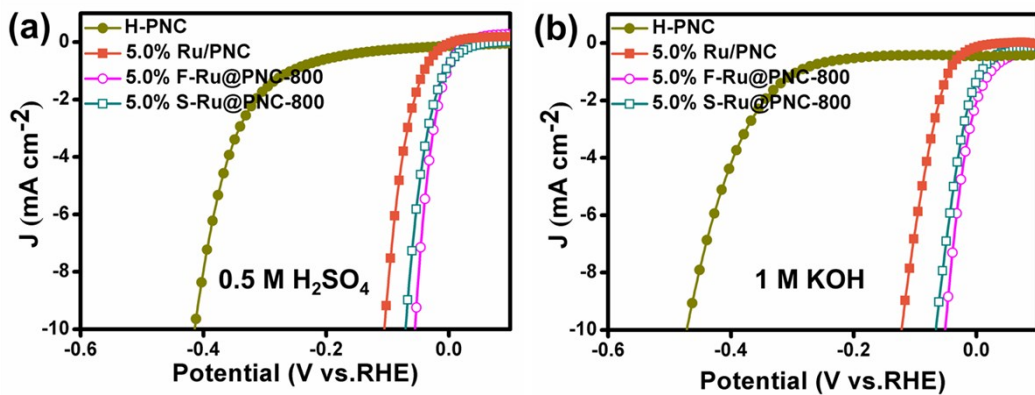


Figure S14. LSV curves of H-PNC, 5.0% Ru/PNC, 5.0% S-Ru@PNC-800, and 5.0% F-Ru@PNC-800 catalysts in (a) 0.5 M H_2SO_4 , (b) 1 M KOH.

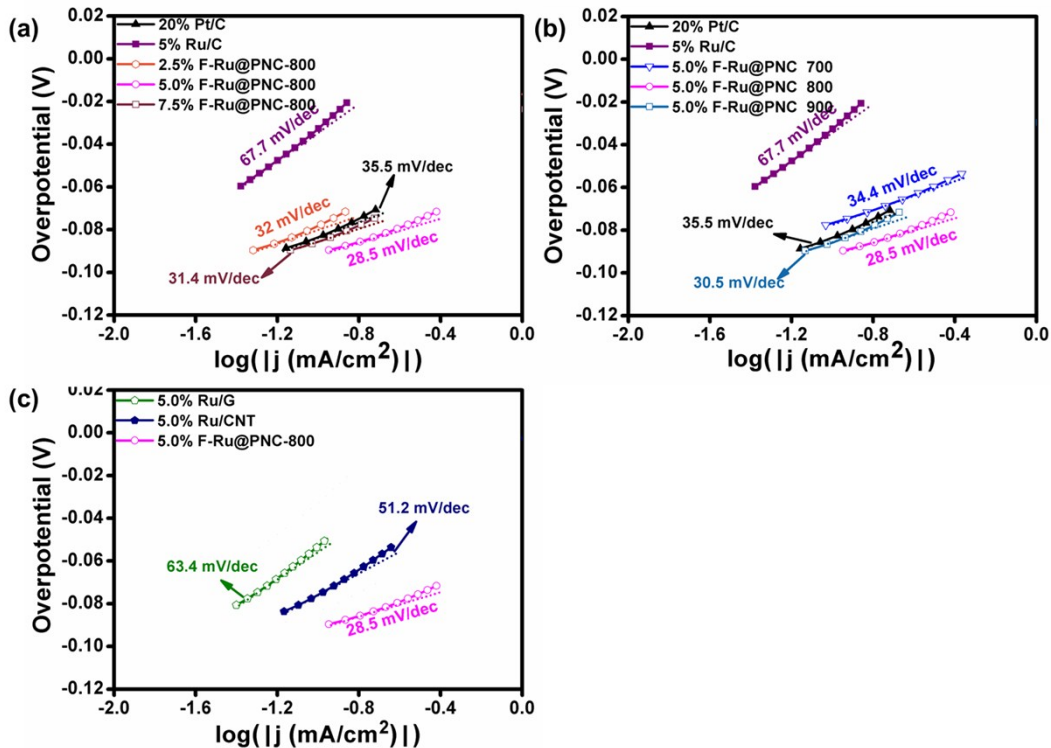


Figure S15. The Tafel plots of (a) F-Ru@PNC-800 at different content, commerce Ru/C and Pt/C in 0.1 M KOH (b) 5.0% F-Ru@PNC samples with different temperatures, commerce Ru/C and Pt/C in 0.1 M KOH (c) 5.0% Ru/G, 5.0% Ru/CNT and 5.0% F-Ru@PNC-800 in 0.1 M KOH.

Table S2. Comparison of HER performance of 5.0% F-Ru@PNC-800 with other metal HER electrocatalysts in alkaline electrolytes.

Catalysts	condition	Current Density(j mA/cm ²)	Overpotential at the corresponding j(mV)	Ref
5.0% F-Ru@PNC (0.16 mg/cm ²)	0.1 M KOH	10	30	This work
Ru/C ₃ N ₄ /C (0.20 mg/cm ²)	0.1 M KOH	10	79	1
Ni(OH) ₂ /Pt/C (TTK) (0.06 mg/cm ²)	0.1 M KOH	10	90	2
WC-CNTs	0.5M H ₂ SO ₄ 0.1 M KOH	10 10	145 137	3
NiOx/Pt ₃ Ni Pt ₃ Ni ₃ -NWs (0.015 mg/cm ²)	0.1 M KOH 1 M KOH	10 10	45 40	4
Pt NWs/SL-Ni(OH) ₂ (0.016 mg/cm ²)	0.1 M KOH 1 M KOH	10 10	48 70	5
Pt	0.1 M KOH	10	30	6
N, P doped-Graphene (0.2 mg/cm ²)	0.5 M H ₂ SO ₄ 0.1 M KOH	10 10	420 570	7
Graphitic-C ₃ N ₄ /N-doped graphene (0.1 mg/cm ²)	0.5 M H ₂ SO ₄ 0.1 M KOH	10 10	240 560	8
np-CuTi	0.1 M KOH	10	47	9
CoMoSx	0.1 M KOH	10	185	10

Table S3. Comparison of HER performance for 5.0% F-Ru@PNC materials and other HER electrocatalysts.

Catalysts ^{a)}	Overpotential (mV)	Tafel slope (mV/dec)	$J_{0,\text{geometrica}}$ ($\mu\text{A cm}^{-2}$) ^{b)}
5.0% F-Ru@PNC-800	30	28.5	89
5.0% S-Ru@PNC-800	72	34.1	81
5.0% Ru/PNC	152	92.2	35
H-PNC	478	161.1	5

a) All the parameters were measured under the same conditions; b) Exchange current densities (j_0) were obtained from Tafel curves by using extrapolation methods.

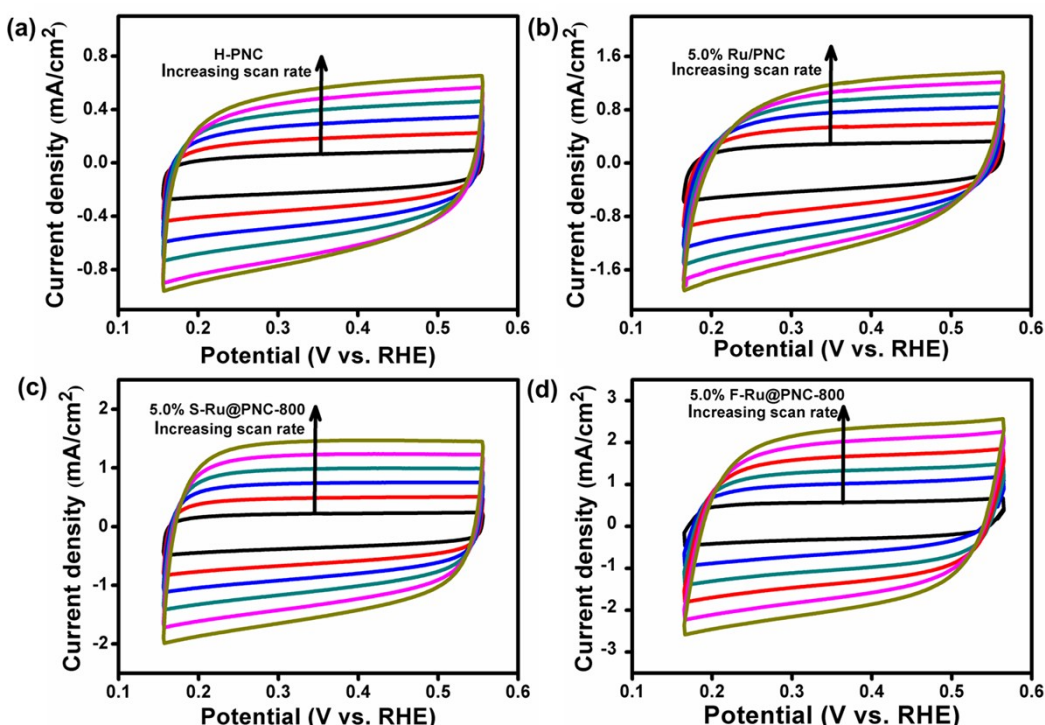


Figure S16. Cyclic voltammograms at different scan rates in the region of 0.165V-0.565mV vs. RHE in 0.1M KOH (a) H-PNC (b) 5.0% Ru/PNC (c) 5.0% S-Ru@PNC-800 (d) 5.0% F-Ru@PNC-800.

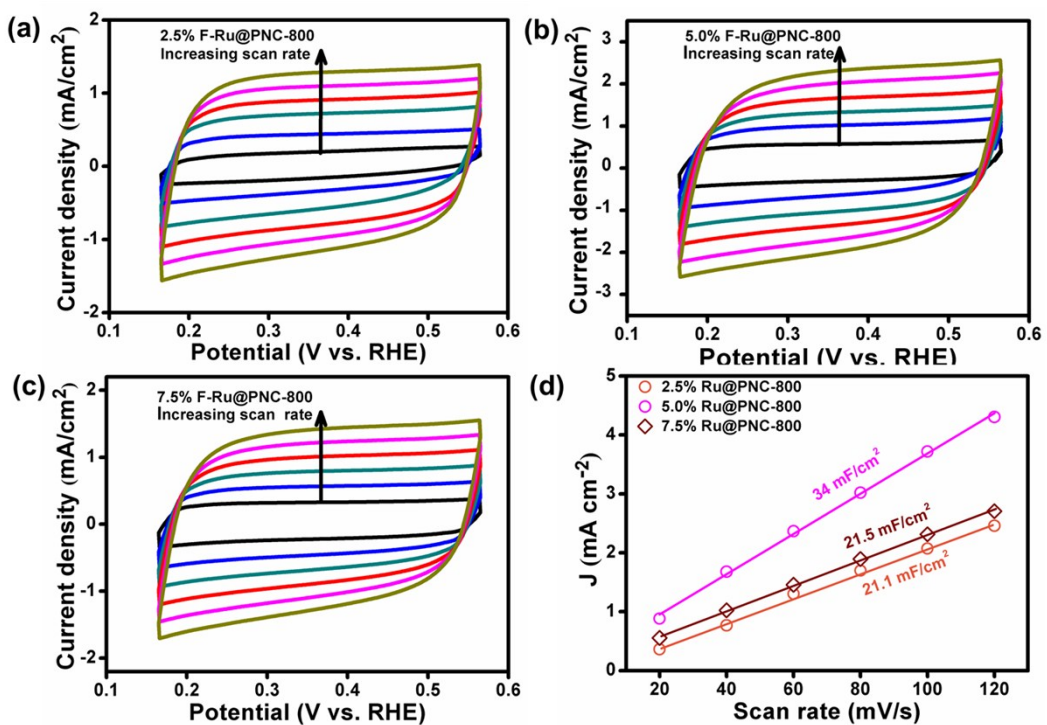


Figure S17. Cyclic voltammograms at different scan rates in the region of 0.165V-0.565mV vs. RHE in 0.1M KOH (a) 2.5% F-Ru@PNC-800 (b) 5.0% F-Ru@PNC-800 (c) 7.5% F-Ru@PNC-800 (d) Charging current density differences plotted against scan rates of 2.5% F-Ru@PNC-800, 5.0% F-Ru@PNC-800 and 7.5% F-Ru@PNC-800.

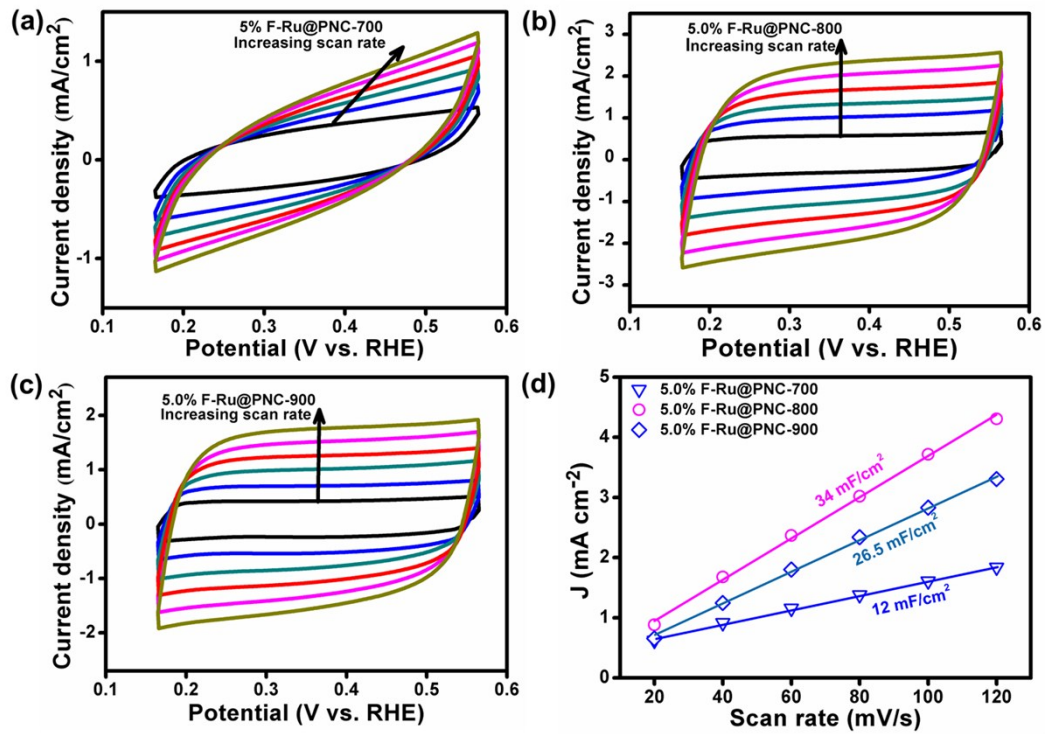


Figure S18. Cyclic voltammograms at different scan rates in the region of 20-120 mV vs. RHE in 0.1M KOH (a) 5.0% F-Ru@PNC-700 (b) 5.0% F-Ru@PNC-800 (c) 5.0% F-Ru@PNC-900 (d) Charging current density differences plotted against scan rates of 5.0% Ru@PNC-700, 5.0% F-Ru@PNC-800 and 5.0% F-Ru@PNC-900.

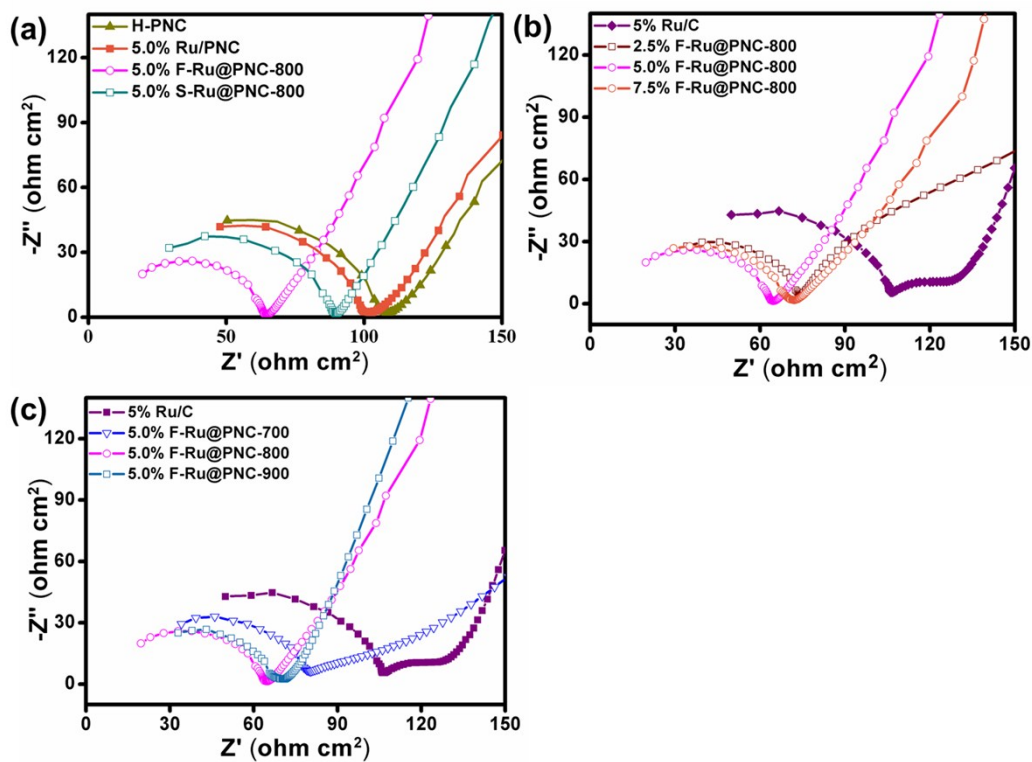


Figure S19. Electrochemical impedance spectroscopy data for (a) H-PNC, 5.0% Ru/PNC, 5.0% S1-Ru@PNC-800, and 5.0% F-Ru@PNC-800 electrocatalysts in 0.1M KOH (b) F-Ru@PNC-800 of different content and 5.0% Ru/C electrocatalysts in 0.1M KOH (c) 5.0% F-Ru@PNC samples with different temperatures and 5.0% Ru/C in 0.1M KOH.

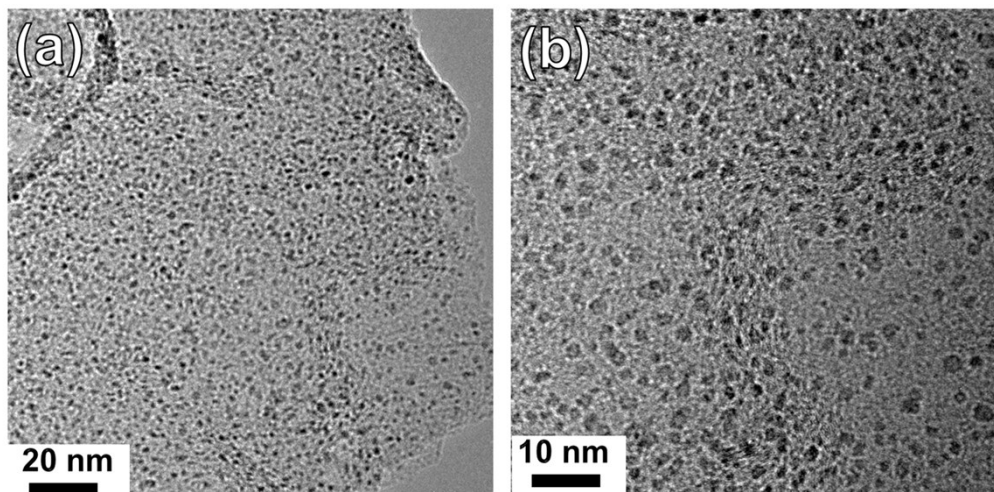


Figure S20. TEM image of used 5.0% F-Ru@PNC-800 after being used for 15h in HER for stability test.

Table S4. The four samples adsorption energy on carbon and ruthenium and the charge transfer number of carbon and ruthenium with hydrogen. Ru_{Eab} and C_{Eab} On behalf of adsorption energy, C_c and Ru_c On behalf of charge transfer number.

Sample	C_{Eab}	C_c	Ru_{Eab}	Ru_c
Ru/PNC	/	/	-0.69	0.8645
Ru@PNC-1	-0.16	0.2859	-0.53	1.3
Ru@PNC-2	-0.36	0.2341	-0.29	1.5175
Ru@PNC-3	-0.52	0.2094	-0.21	1.8246

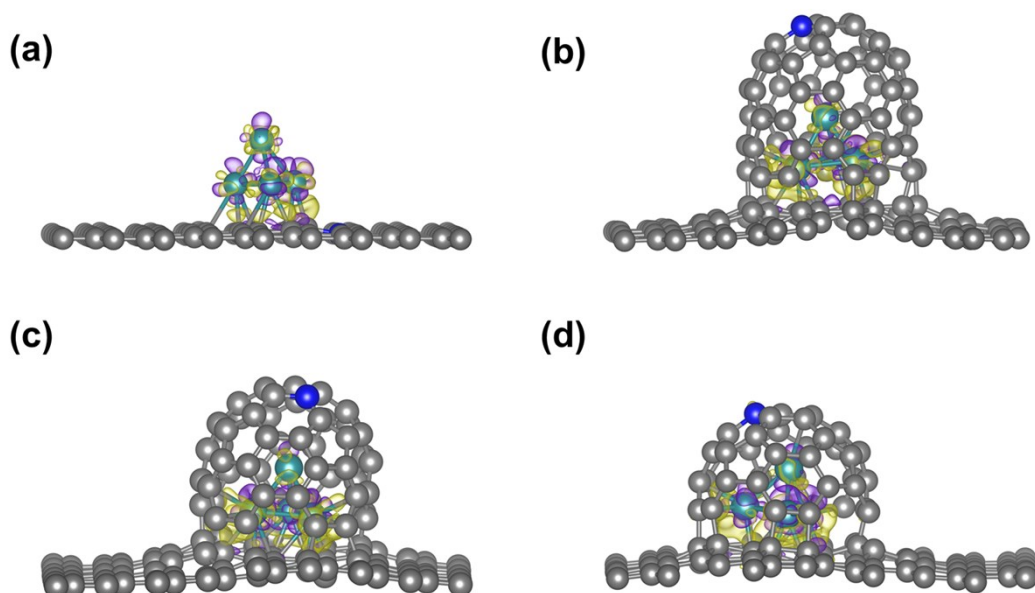


Figure S21. The charge density differences of (a) Ru/PNC (b) Ru@PNC-1 (c) Ru@PNC-2 (d) Ru@PNC-3. Grey, blue, white and green represents carbon, nitrogen, hydrogen and ruthenium. Purple and yellow represent positive and negative charges, respectively.

Table S5. The charge transfer number of ruthenium. Ru_c On behalf of charge transfer number.

Sample	Ru_c
Ru/PNC	0.5788
Ru@PNC-1	1.2425
Ru@PNC-2	1.3213
Ru@PNC-3	1.6106

References

1. Y. Zheng, Y. Jiao, Y. H. Zhu, L. H. Li, Y. Han, Y. Chen, M. Jaroniec and S. Z. Qiao, *J. Am. Chem. Soc.*, 2016, **138**, 16174-16181.
2. R. Subbaraman, D. Tripkovic, D. Strmcnik, K. C. Chang, M. Uchimura, A. P. Paulikas, V. Stamenkovic and N. M. Markovic, *Science*, 2011, **334**, 1256-1260.
3. X. J. Fan, H. Q. Zhou and X. Guo, *ACS Nano*, 2015, **9**, 5125-5134.
4. P. T. Wang, K. Z. Jiang, G. M. Wang, J. L. Yao and X. Q. Huang, *Angew. Chem. Int. Ed.*, 2016, **55**, 12859-12863.
5. H. J. Yin, S. L. Zhao, K. Zhao, A. Muqsit, H. J. Tang, L. Chang, H. J. Zhao, Y. Gao and Z. Y. Tang, *Nat. Commun*, 2015, **6**, 7430.
6. W. C. Sheng, M. Myint, J. G. G. Chen and Y. S. Yan, *Energy Environ. Sci.*, 2013, **6**, 1509-1512.
7. Y. Zheng, Y. Jiao, L. H. Li, T. Xing, Y. Chen, M. Jaroniec and S. Z. Qiao, *ACS Nano*, 2014, **8**, 5290-5296.
8. Y. Zheng, Y. Jiao, Y. H. Zhu, L. H. Li, Y. Han, Y. Chen, A. J. Du, M. Jaroniec and S. Z. Qiao, *Nat. Commun*, 2014, **5**, 4783.
9. Q. Lu, G. S. Hutchings, W. T. Yu, Y. Zhou, R. V. Forest, R. Z. Tao, J. Rosen, B. T. Yonemoto, Z. Y. Cao, H. M. Zheng, J. Q. Xiao, F. Jiao and J. G. G. Chen, *Nat. Commun*, 2015, **6**, 7567.
10. J. Staszak-Jirkovsky, C. D. Malliakas, P. P. Lopes, N. Danilovic, S. S. Kota, K. C. Chang, B. Genorio, D. Strmcnik, V. R. Stamenkovic, M. G. Kanatzidis and N. M. Markovic, *Nat. Mater.*, 2016, **15**, 197-184.